J|A|C|S ARTICLES

Published on Web 08/24/2009

# Mechanism of Ethanol Synthesis from Syngas on Rh(111)

YongMan Choi and Ping Liu*

*Chemistry Department, Brookhaven National Laboratory, Upton, New York, 11973*

Received April 15, 2009; E-mail: pingliu3@bnl.gov

***Abstract:*** Rh-based catalysts display unique efficiency and selectivity in catalyzing ethanol synthesis from syngas ($2CO + 4H_2 \rightarrow C_2H_5OH + H_2O$). Understanding the reaction mechanism at the molecular level is the key to rational design of better catalysts for ethanol synthesis, which is one of major challenges for ethanol application in energy. In this work, extensive calculations based on density functional theory (DFT) were carried out to investigate the complex ethanol synthesis on Rh(111). Our results show that ethanol synthesis on Rh(111) starts with formyl formation from CO hydrogenation, followed by subsequent hydrogenation reactions and CO insertion. Three major products are involved in this process: methane, methanol, and ethanol, where the ethanol productivity is low and Rh(111) is highly selective to methane rather than ethanol or methanol. The rate-limiting step of the overall conversion is the hydrogenation of CO to formyl species, while the selectivity to ethanol is controlled by methane formation and C−C bond formation between methyl species and CO. The strong Rh−CO interaction impedes the CO hydrogenation and therefore slows down the overall reaction; however, its high affinity to methyl, oxygen, and acetyl species indeed helps the C−O bond breaking of methoxy species and therefore the direct ethanol synthesis via CO insertion. Our results show that to achieve high productivity and selectivity for ethanol, Rh has to get help from the promoters, which should be able to suppress methane formation and/or boost C−C bond formation. The present study provides the basis to understand and develop novel Rh-based catalysts for ethanol synthesis.

## I. Introduction

The finite resources of fossil fuels along with environmental concerns have stimulated a broad intensive search for alternative energy sources.[1,2] As a fuel,[3,4] ethanol has several ideal properties: it is nontoxic, easy to store and transport, producible from renewable sources, and has a high energy density comparable to that of gasoline. One of the major obstacles for ethanol application in energy is the slow kinetics and low selectivity in ethanol synthesis. Developing catalysts for synthesizing ethanol efficiently and selectively has been one of the major challenges in catalysis.

Rh-based catalysts promoted by certain promoters and/or reducible metal oxides[5−7] have been found to display unique efficiency and selectivity in catalyzing ethanol synthesis from syngas ($2CO + 4H_2 \rightarrow C_2H_5OH + H_2O$), one of the major ethanol production processes in industry. Rh-based catalysts are by far the most studied systems for ethanol synthesis and are the only group of materials that convert syngas directly into ethanol, rather than via methanol.[5,6] However, few studies have been carried out to understand the ethanol synthesis on Rh-based catalysts at the fundamental level due to the complexity of the reactions. So far, there is no generally accepted mechanism. An alternative involves CO dissociation and insertion initiated by $H_2$ and CO adsorption.[5−7] Nondissociated CO is hydrogenated to form methanol ($CH_3OH$), while dissociated CO is then hydrogenated to produce surface hydrocarbon species ($CH_x$). $CH_x$ either undergoes hydrogenation to produce methane ($CH_4$) or forms $C_2$ oxygenates by CO insertion, which is eventually hydrogenated to form $C_2H_5OH$. Extensive experiments have been carried out to investigate the roles of promoters and supports, showing that a good promoter or a support may help the CO dissociation and insertion while suppressing the $CH_x$ hydrogenation.[5−7] Yet, actual mechanisms are unclear: What is the rate-limiting step (rls)? What is the selectivity-controlling step (scs)? Why does Rh have to be the base material? What is the role of Rh?

In this study, we employed density functional theory (DFT) to investigate ethanol synthesis on Rh(111) from syngas, aiming to identify plausible reaction mechanisms, determine the kinetics, and understand the role of Rh in this process. In fact, Rh(111) has been chosen as a model system to study hydrocarbon combustion,[8−10] as Rh-based catalysts also display superior activity for the reverse conversion, ethanol oxidation.[4,11,12] Our results show that ethanol synthesis on Rh(111) is initiated with CO hydrogenation to formyl (HCO). In contrast, CO

(1) Song, C. *Catal. Today* **2006**, *115*, 2–32.
(2) Henrici-Olivé., G.; Olivé, S. *Angew. Chem., Int. Ed.* **1976**, *15*, 136–141.
(3) Wang, H.-F.; Liu, Z.-P. *J. Am. Chem. Soc.* **2008**, *130*, 10996–11004.
(4) Kowal, A.; Li, M.; Shao, M.; Sasaki, K.; Vukmirovic, M. B.; Zhang, J.; Marinkovic, N. S.; Liu, P.; Frenkel, A. I.; Adzic, R. R. *Nat. Mater.* **2009**, *8*, 325–330.
(5) Subramani, V.; Gangwal, S. K. *Energy Fuels* **2008**, *22*, 814–839.
(6) Spivey, J. J.; Egbebi, A. *Chem. Soc. Rev.* **2007**, *36*, 1514–1528.
(7) He, J.; Zhang, W.-n. *J. Zhejiang Univ. Sci.* **2008**, *9*, 714–719.
(8) Inderwildi, O. R.; Jenkins, S. J.; King, D. A. *J. Am. Chem. Soc.* **2007**, *129*, 1751–1759.
(9) Inderwildi, O. R.; Jenkins, S. J.; King, D. A. *Angew. Chem., Int. Ed.* **2008**, *47*, 5253–5255.
(10) Wilson, J. N.; Pedigo, R. A.; Zaera, F. *J. Am. Chem. Soc.* **2008**, *130*, 15796–15797.
(11) Idriss, H. *Platinum Met. Rev.* **2004**, *48*, 105–115.


10.1021/ja903013x CCC: $40.75 

***Table 1.*** Adsorption Energies[a] and Geometrical Configurations of Surface Species on Rh(111)

| species | adsorption energy (eV) this study | lit. calc | lit. expt | adsorption configuration |
|---|---|---|---|---|
| C | −7.15 | −7.11[b] | | hcp[b] |
| H | −2.74 | −2.79[b] | −2.66[e] | fcc[b] |
| O | −5.29 | −4.88[b] | | fcc[b] |
| CO | −1.77 (−1.70) | −2.04[b], −1.80[c] | −1.65[f] | atop-bound through C[b,c,f] |
| CH | −6.62 | −6.76[i], −6.54[j] | | hcp-bound through C[i,j] |
| $CH_2$ | −4.14 | | | hcp-bound through C |
| $CH_3$ | −1.90 | −1.84[b] | | atop-bound through C[b] |
| $CH_4$ | 0.00 | | | no adsorption |
| HCO | −2.35 | | | bridge-bound through C[g,h] |
| COH | −4.54 | | | hcp-bound through C |
| CHOH | −2.96 | | | bridge-bound through C |
| $CH_2OH$ | −1.74 | | | atop-bound through C |
| $CH_2O$ | −0.68 | | | fcc-bound through C; atop-bound through O |
| $CH_3O$ | −2.30 | | | fcc-bound through C |
| $CH_3CO$ | −2.41 | | | atop-bound through α-C |
| $CH_3OH$ | −0.28 (−0.25) | | | atop-bound through O |
| $CH_3CHO$ | −0.06 (−0.06) | | | atop-bound through H of α-C |
| $CH_3COH$ | −2.66 | | | atop-bound through α-C |
| $CH_3CHOH$ | −1.52 | | | atop-bound through α-C |
| $CH_3CH_2OH$ | −0.28 (−0.26) | −0.36[d] | | atop-bound through O[d] |
| $H_2O$ | −0.33 (−0.27) | | | atop-bound through O |

[a] Values in parentheses are ZPE-corrected. [b] Reference 19. [c] Reference 26. [d] Reference 27. [e] Reference 28. [f] Reference 24. [g] Reference 8. [h] Reference 9. [i] Reference 29. [j] Reference 30.

dissociation on Rh(111) is highly activated. In accordance with the experiments on Rh-based catalysts,[5,6,13] three major products are involved in this process: $CH_4$, $CH_3OH$, and $C_2H_5OH$. However, the $C_2H_5OH$ productivity on Rh(111) is low and it is highly selective to $CH_4$ rather than $C_2H_5OH$. The rls of the overall reaction is the hydrogenation of CO to HCO. The scs to $C_2H_5OH$ is controlled by $CH_4$ formation and by CO insertion or C−C bond formation between methyl ($CH_3$) and CO. The strong Rh−CO interaction is an obstacle to CO hydrogenation and therefore the overall conversion; however, its high affinity to $CH_3$, O, and acetyl ($CH_3CO$) indeed helps break the C−O bond of $CH_3O$ and make direct ethanol synthesis possible. Our results show that, to achieve high productivity and selectivity for $C_2H_5OH$, Rh has to get help from the promoters, which should be able to suppress $CH_4$ formation and/or boost C−C bond formation.

## II. Computational Method

Plane-wave DFT calculations with the projector-augmented wave (PAW) method[14] were carried out as implemented in the Vienna ab initio simulation package (VASP).[15,16] The generalized gradient approximation with the Perdew−Wang[17] exchange−correlation functional (GGA-PW91) was used. The kinetic energy cutoff for a plane wave basis set was 400 eV. We applied Monkhorst−Pack[18] mesh **k**-points of (3 × 3 × 3) and (4 × 4 × 1) for bulk and surface calculations, respectively, allowing convergence to 0.01 eV of the total electronic energy. The calculated equilibrium lattice constant for Rh is 3.843 Å, which agrees well with theoretical[19] and experimental[20] values (3.83 and 3.797 Å, respectively). For the 2-D slab model calculations, three-layer p(2 × 2) Rh(111) surfaces similar to a previous study[19] were separated by a vacuum space equivalent to four layers in the direction perpendicular to the surface. We tested that there is no significant effect on the energetics by increasing the number of layers up to 5. Spin-polarization calculations were carried out. The reaction pathways of the syngas interactions on Rh(111) were investigated by the climbing-image nudged elastic band method (CI-NEB).[21,22] Transition states were identified by the number of imaginary frequencies (NIMG) with NIMG = 1. Zero-point energy (ZPE) corrections are included for final potential energy diagrams and microkinetic modeling. We applied the transition-state theory (TST) formalism[23] to predict rate constants for elementary steps.

## III. Results and Discussion

**A. Adsorptions of Reactants and Possible Intermediates.** Adsorptions of the reactants and all possible intermediates involved in ethanol synthesis on Rh(111) were considered. The preferential adsorption morphologies and corresponding adsorption energies are listed in Table 1. According to our DFT calculations, CO on Rh(111) at coverage of 0.25 monolayer (ML) preferentially occupies the atop site with a binding energy as strong as −1.77 eV (see Table 1), which agrees well with the experiments[24,25] and other calculations at a similar level of theory.[19,26] We found that the adsorption energy after a ZPE correction (−1.70 eV) is in better agreement with the experimental value of −1.65 eV.[24] Thus we will use the ZPE-corrected energies for constructing final energy diagrams and carrying

(12) Idriss, H.; Scott, M.; Llorca, J.; Chan, S. C.; Chiu, W.; Sheng, P.-Y.; Yee, A.; Blackford, M. A.; Pas, S. J.; Hill, A. J.; Alamgir, F. M.; Rettew, R.; Petersburg, C.; Senanayake, S. D.; Barteau, M. A. *ChemSusChem* **2008**, *1*, 905–910.
(13) Haider, M. A.; Gogate, M. R.; Daivs, R. J. *J. Catal.* **2009**, *261*, 9–16.
(14) Blöchl, P. E. *Phys. Rev. B* **1994**, *50*, 17953–17979.
(15) Kresse, G.; Hafner, J. *Phys. Rev. B* **1993**, *47*, 558.
(16) Kresse, G.; Furthmüller, J. *Phys. Rev. B* **1996**, *54*, 11169.
(17) Perdew, J. P.; Burke, K.; Ernzerhof, M. *Phys. Rev. Lett.* **1996**, *77*, 3865–3868.
(18) Monkhorst, H. J.; Pack, J. D. *Phys. Rev. B* **1976**, *13*, 5188–5192.
(19) Mavrikakis, M.; Rempel, J.; Greeley, J.; Hansen, L. B.; Nørskov, J. K. *J. Chem. Phys.* **2002**, *117*, 6737–6744.
(20) *CRC Handbook of Chemistry and Physics*, 76th ed.; Lide, D. R., Ed.; CRC Press: New York, 1996.
(21) Henkelman, G.; Jónsson, H. *J. Phys. Chem.* **2000**, *113*, 9978–9985.
(22) Henkelman, G.; Uberuaga, B. P.; Jónsson, H. *J. Phys. Chem.* **2000**, *113*, 9901–9904.
(23) Laidler, K. J. *Chemical Kinetics*, 3rd ed.; Harper and Row: New York, 1987.
(24) Hopstaken, M. J. P.; Niemantsverdriet, J. W. *J. Chem. Phys.* **2000**, *113*, 5457–5465.
(25) Beutler, A.; Lundgren, E.; Nyholm, R.; Andersen, J. N.; Setlik, B.; Heskett, D. *Surf. Sci.* **1997**, *371*, 381–389.
(26) Zhang, C. J.; Hu, P.; Lee, M.-H. *Surf. Sci.* **1999**, *432*, 305–315.

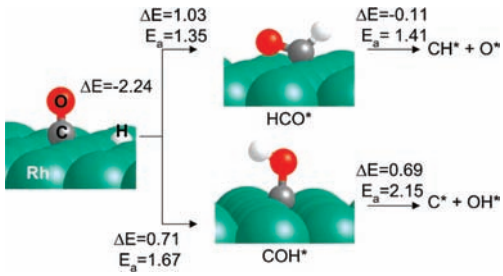


***Figure 1.*** Formation and dissociation of formyl species on Rh(111) (large cyan, Rh; small red, O; small gray, C; small white, H). Reaction barriers ($E_a$) and heat of reactions ($\Delta E$) are in electronvolts. An asterisk denotes a surface site.

out the following kinetic modeling. For the geometrical parameters, the estimated distances of Rh−C and C−O are in excellent agreement with the experimental results[31] (1.854 and 1.164 Å vs 1.84 ± 0.07 and 1.15 ± 0.07 Å, respectively). Similar agreements between the present calculations and available literature data are also observed for C, H, O, and $CH_x$ ($x$ = 1−3) and $C_2H_5OH$ (see Table 1). All optimized geometries and calculated energies are summarized in Tables S1−S3 in the Supporting Information.

**B. Reaction Pathways.** We also carried out DFT calculations to explore $C_2H_5OH$ synthesis on the Rh(111) surface. The overall reaction is highly exothermic [$\Delta H^o(298\ K) = -2.63$ eV],[5] indicating that direct $C_2H_5OH$ formation is thermodynamically favorable. Therefore, the conversion is merely inhibited by kinetics. As shown in the following, multiple reaction paths were considered in the present DFT study, and on this basis, an optimal pathway will be identified.

**B.1. Carbon Monoxide Dissociation and Hydrogenation to Methoxy.** As mentioned before, one of the crucial elementary reaction steps for $C_2H_5OH$ synthesis on Rh-based catalysts is CO dissociation. It has been reported[5−7] that only dissociated CO can lead to the formation of ethanol; otherwise, only methanol is produced. Our DFT calculations found that a barrier for CO dissociation on Rh(111) surfaces is 3.72 eV, in accordance with previous studies.[32−35] In addition, it was also found that the low index steps indeed help lower the dissociation barrier compared to the flat surface; yet C−O bond cleavage is very difficult to achieve.[32,36] That is, the CO dissociation pathway is very unlikely on Rh(111).

In contrast, the hydrogenation of CO to formyl species (COH or HCO) is more plausible. As shown in Figure 1, the barriers for forming COH and HCO are 1.67 and 1.35 eV, respectively.

***Table 2.*** Reaction Mechanisms, Prefactors Calculated at 543 K, and Reaction Barriers ($E_a$) Used for Microkinetic Modeling[a]

| | process | prefactor ($s^{-1}$) | $E_a$ (eV) |
|---|---|---|---|
| **R1** | $CO(g) + * \leftrightarrow CO*$ | | |
| **R2** | $H_2(g) + 2* \leftrightarrow 2H*$ | | |
| **R3** | $CO* + H* \rightarrow HCO* + *$ | $2.0 \times 10^{12}$ | 1.28 |
| **R4** | $HCO* + H* \rightarrow CH_2O* + *$ | $2.5 \times 10^{12}$ | 0.42 |
| **R5** | $CH_2O* + H* \rightarrow CH_3O* + *$ | $2.2 \times 10^{13}$ | 0.72 |
| **R6** | $CH_3O* + H* \rightarrow CH_3OH(g) + 2*$ | $6.9 \times 10^{11}$ | 0.76 |
| **R7** | $CH_3O* + * \rightarrow CH_3* + O*$ | $1.6 \times 10^{15}$ | 1.05 |
| **R8** | $CH_3* + H* \rightarrow CH_4(g) + 2*$ | $3.8 \times 10^{13}$ | 0.80 |
| **R9** | $CH_3* + CO* \rightarrow CH_3CO* + *$ | $6.8 \times 10^{11}$ | 1.15 |
| **R10** | $CH_3CO* + H* \rightarrow CH_3CHO(g) + 2*$ | $4.3 \times 10^{12}$ | 1.12 |
| **R11** | $CH_3CO* + H* \rightarrow CH_3COH* + *$ | $1.0 \times 10^{14}$ | 0.82 |
| **R12** | $CH_3COH* + H* \rightarrow CH_3CHOH* + *$ | $2.5 \times 10^{13}$ | 0.69 |
| **R13** | $CH_3CHOH* + H* \rightarrow CH_3CH_2OH(g) + 2*$ | $1.2 \times 10^{13}$ | 0.45 |
| **R14** | $O* + H* \rightarrow OH* + *$ | $5.7 \times 10^{13}$ | 1.03 |
| **R15** | $OH* + H* \rightarrow H_2O(g) + *$ | $1.5 \times 10^{13}$ | 0.37 |

[a] An asterisk represents a free site on the surface.

Both reactions are more favorable than CO dissociation, and HCO formation is more preferred. Therefore, the adsorbed CO species on Rh(111) undergoes hydrogenation to form HCO (**R3**, Table 2). In fact, formyl species have been recognized in many reactions associated with CO hydrogenation. Deluzarche et al.[37] summarized a plausible pathway to produce ethanol via formyl species (COH and HCO) on Rh/$TiO_2$. In addition, experiments using the chemical trapping approach proposed the significance of formyl species for alcohol synthesis on Rh/$SiO_2$ catalysts containing $CeO_2$[38] and Li-promoted Pd/$CeO_2$.[39] Remediakis et al.[40] reported that formyl species are important intermediates involved in methanol synthesis from CO and $H_2$ on Ni(111).

There are two possibilities for the further reaction of HCO: one is hydrogenation to form hydroxymethylene (HCOH) or formaldehyde ($CH_2O$) species; the other is dissociation into CH and O. Again hydrogenation is superior to dissociation. As shown in Figure 2, the HCO intermediate can be more easily hydrogenated by adding one hydrogen atom to carbon and forming $CH_2O$ (**R4**, Table 2) than its dissociation. The corresponding reaction barriers are 0.48 eV versus 1.41 eV.

Similarly, $CH_2O$ prefers to be hydrogenated rather than being dissociated into $CH_2$ and O (see Figure 2). A high barrier of 1.43 eV is obtained for $CH_2O$ dissociation, while the barriers of 0.68 and 0.83 eV are calculated for the formation of methoxy ($CH_3O$, **R3**, Table 2) and hydroxymethyl ($CH_2OH$) species, respectively. Therefore, $CH_2$ formation from $CH_2O$ seems unlikely. In addition, one can see in Figure 2 that the production of $CH_3O$ is preferred rather than that of $CH_2OH$, not only due to the lower formation barrier by 0.15 eV but also associated with a higher stability on Rh(111) by 0.21 eV. The high stability of $CH_3O$ on Rh(111) is attributed to its oxygen moiety, which occupies the 3-fold fcc site, similar to a previous study on Ni(111).[40] Given that, we conclude that CO → HCO → $CH_2O$ → $CH_3O$ (**R1, R3−R5**, Table 2) is an optimal pathway for the initial CO hydrogenation on Rh(111).

**B.2. Methanol, Methane, and Ethanol Production from Methoxy Species.** As depicted in Figure 2, compared to the cases

(27) Yang, M.-M.; Bao, X.-H.; Li, W.-Z. *J. Phys. Chem. C* **2007**, *111*, 7403–7410.
(28) Yates, J. T., Jr.; Thiel, P. A.; Weinberg, W. H. *Surf. Sci.* **1979**, *82*, 427–439.
(29) Bunnik, B. S.; Kramer, G. J. *J. Catal.* **2006**, *242*, 309–318.
(30) Resta, A.; Gustafson, J.; Westerström, R.; Mikkelsen, A.; Lundgren, E.; Andersen, J. N.; Yang, M.-M.; Ma, X.-F.; Bao, X.-H.; Li, W.-X. *Surf. Sci.* **2008**, *602*, 3057–3063.
(31) Gierer, M.; Barbieri, A.; Hove, M. A. V.; Somorjai, G. A. *Surf. Sci.* **1997**, *391*, 176–182.
(32) Mavrikakis, M.; Bäumer, M.; Freund, H.-J.; Nørskov, J. K. *Catal. Lett.* **2002**, *81*, 153–156.
(33) Castner, D. G.; Sexton, B. A.; Somorjai, G. A. *Surf. Sci.* **1978**, *71*, 519–540.
(34) Thiel, P. A.; Williams, E. D.; Yates, J. T., Jr.; Weinberg, W. H. *Surf. Sci.* **1979**, *84*, 54–64.
(35) Stroppa, A.; Mittendorfer, F.; Andersen, J. N.; Parteder, G.; Allegretti, F.; Surnev, S.; Netzer, F. P. *J. Phys. Chem. C* **2009**, *113*, 942–949.
(36) Batteas, J. D.; Gardin, D. E.; Hove, M. A. V.; Somorjai, G. A. *Surf. Sci.* **1993**, *297*, 11–18.
(37) Deluzarche, A.; Hindermann, J. P.; Kieffer, R.; Breault, R.; Kiennemann, A. *J. Phys. Chem.* **1984**, *88*, 4993–4995.
(38) Kiennemann, A.; Breault, R.; Hindermann, J.-P.; Laurin, M. *J. Chem. Soc., Faraday Trans. 1* **1987**, *83*, 2119–2128.
(39) Diagne, C.; Idriss, H.; Hindermann, J. P.; Kiennemann, A. *Appl. Catal.* **1989**, *51*, 165–180.
(40) Remediakis, I. N.; Abild-Pedersen, F.; Nørskov, J. K. *J. Phys. Chem. B* **2004**, *108*, 14535–14540.

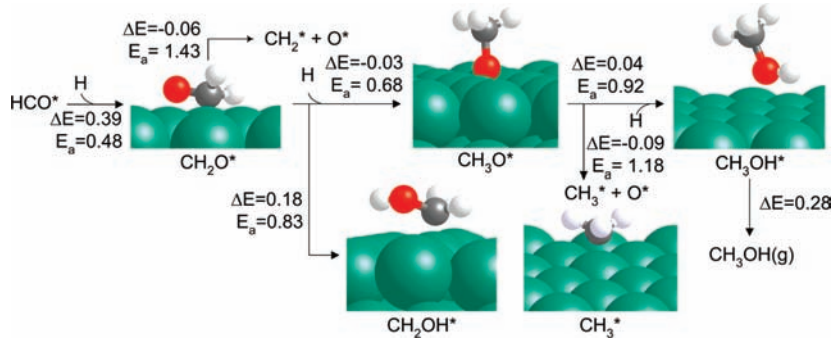


***Figure 2.*** Hydrogenation, dissociation of $CH_3O$ species, and methanol formation on Rh(111) (large cyan, Rh; small red, O; small gray, C; small white, H). Reaction barriers ($E_a$) and heat of reactions ($\Delta E$) are in electronvolts.An asterisk denotes a surface site.

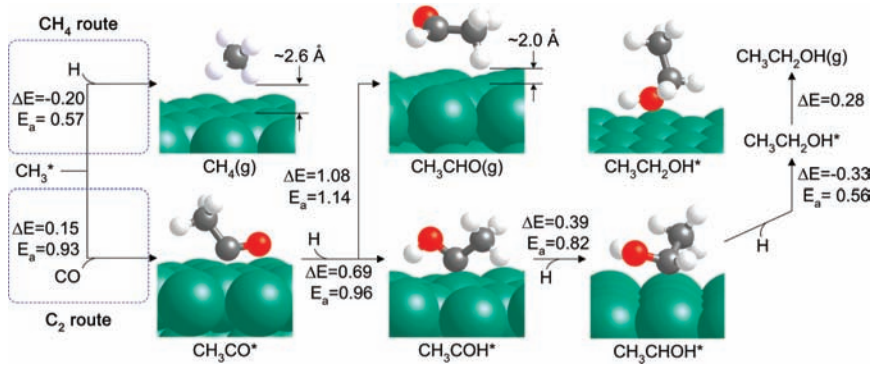


***Figure 3.*** Methane and ethanol formation on Rh(111) (large cyan, Rh; small red, O; small gray, C; small white, H). Reaction barriers ($E_a$) and heat of reactions ($\Delta E$) are in electronvolts. An asterisk denotes a surface site. "$C_2$ route" represents the reaction pathways forming species with one C−C bond.

of HCO and $CH_2O$, the dissociation of $CH_3O$ process (**R7**, Table 2) is energetically compatible with the hydrogenation (**R6**, Table 2). A barrier for C−O bond breaking of $CH_3O$ is 1.18 eV, which is only 0.26 eV higher than that of $CH_3O$ hydrogenation. Besides, the heat of reaction only differs by 0.05 eV. Therefore, both steps were considered in our study. $CH_3O$ hydrogenation leads to the production of $CH_3OH$ (see Figure 2), which quickly desorbs from the surface with a barrier of only 0.28 eV. When the dissociation occurs, $CH_3$ is formed with the produced O atom removed from the surface in the form of $H_2O$ (**R14** and **R15,** Table 2). Note that the water−gas shift (WGS) reaction ($CO + H_2O \rightarrow CO_2 + H_2$) was not included here. It has already been found that the WGS reaction is highly activated on Rh(111).[43]

$CH_4$ was then produced by hydrogenating the $CH_3$ species (**R8**, Table 2) and its corresponding barrier is 0.57 eV (see Figure 3). Once $CH_4$ is formed, it does not stick to Rh(111) and desorbs immediately (see Table 1). As depicted in Figure 3, an alternative route includes the insertion of CO to $CH_3$ (**R9**, Table 2). It has been found that the chain growth or C−C bond formation is a very difficult process during alcohol synthesis.[5−7] The formal charge on the methyl group is −1, which implies that two electrons occupy the $\sigma$-symmetric lone pair orbital. When the $CH_3$ fragment migrates to CO and a C−C bond is formed, the doubly occupied $5\sigma$ CO orbital interacts with the doubly occupied $\sigma$-$CH_3$ orbitals, resulting in doubly occupied bonding and antibinding orbitals, giving the repulsive interaction. According to our density of states (DOS) calculations for the $CH_3CO$ formation process (Figure S1 in Supporting Information), the empty d orbitals of Rh can accept electrons from CO and $CH_3$ fragment orbitals, thus reducing the repulsion and making C−C bond formation easier. The corresponding barrier is 0.93 eV. One can see that the hydrogenation and CO insertion processes compete for the $CH_3$ species. Obviously on Rh(111), $CH_4$ formation is faster than $CH_3CO$ formation in terms of the reaction barrier. It will be shown in the following section that pure Rh(111) is highly selective to the $CH_4$ production, rather than $CH_3OH$ and $C_2H_5OH$.

In fact, we also considered the $CH_3$ dissociation to $CH_2$, as $CH_x$ species ($x$ = 1, 2, or 3) have been proposed as crucial intermediates in ethanol synthesis.[5−7] In addition, we also examined a plausible route forming a C−C bond formation via $CH_2 + CO$. We located a transition state for $CH_3 \rightarrow CH_2 + H$. The corresponding barrier is 0.54 eV, while that for $CH_2 + H \rightarrow CH_3$ is 0.49 eV. According to our microkinetic modeling as shown below, under typical experimental conditions ($P_{CO}$ = 4 atm, $P_{H_2}$ = 8 atm, and $T$ = 543 K), a surface coverage of H is approximately $10^4$ times larger than those of $CH_3$ and $CH_2$, which will overpass the small difference in barrier and facilitate $CH_2 + H \rightarrow CH_3$, rather than the reverse. In addition, a recent study[41] has shown that $CH_2 + CO \rightarrow CH_2CO$ on Rh(111) is highly activated with a barrier of 1.34 eV,[42] which cannot compete with $CH_2$ hydrogenation. Thus, the possibilities of $CH_2$ formation and of CO insertion via $CH_2$ are ruled out from the optimal pathway.

For $CH_3CO$ hydrogenation, there are two possible products. One is $CH_3CHO$, which is produced by overcoming a barrier of 1.14 eV (**R10**, Table 2) and desorbs immediately via a barrier

(41) Ferrin, P.; Simonetti, D.; Kandoi, S.; Kunkes, E.; Dumesic, J. A.; Nørskov, J. K.; Mavrikakis, M. *J. Am. Chem. Soc.* **2009**, *131*, 5809–5815.

(42) The barrier was provided by the authors of ref 41 through a personal communication.

(43) Burch, R.; Petch, M. I. *Appl. Catal., A* **1992**, *88*, 39–60.

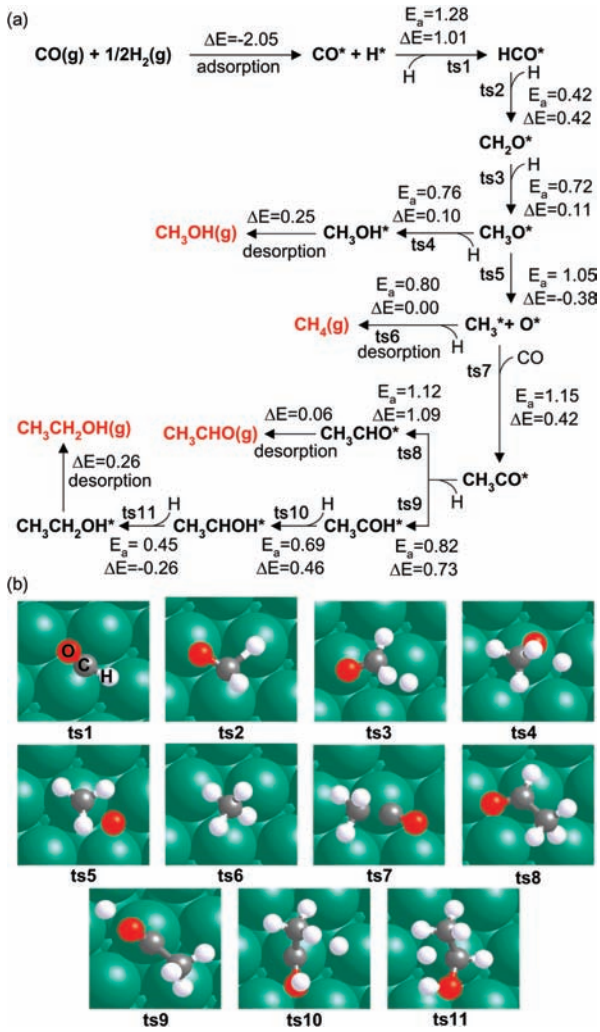


***Figure 4.*** (a) Schematic of the optimal reaction pathway for $C_2H_5OH$ synthesis from CO and $H_2$ on Rh(111), where both reaction barriers ($E_a$) and heat of reactions ($\Delta E$) are ZPE-corrected and in the unit of electronvolts. (b) Top view of transition states involved in the reaction shown in panel a (large cyan, Rh; small red, O; small gray, C; small white, H). Corresponding geometries for the intermediates are shown in Figures 1−3.

of 0.06 eV. Burch and Petch[43] reported that $CH_3CHO$ species on supported Rh catalysts can produce ethanol via a subsequent hydrogenation; however our calculations on Rh(111) show that $CH_3CHO$ is formed as a byproduct. In contrast, the formation of $CH_3COH$ (**R11**, Table 2) is slightly more favorable (see Figure 3, 1.14 vs 0.96 eV). Eventually, $C_2H_5OH$ is produced via $CH_3COH$ by hydrogenating at the α-carbon site and then easily desorbs via a barrier of 0.28 eV. It has been reported[44,45] that the oxametallacycle species ($CH_2CH_2O$) is the most plausible reaction intermediate of the decomposition reaction of ethanol on a $CeO_2$(111)-supported Rh cluster. This species, however, is not favored for the reverse, ethanol synthesis, on Rh(111) according to our calculations. In our optimal reaction mechanism (Figure 4), the precursors for the C−C bond formation are $CH_3$ and CO. The sequential hydrogenations of $CH_3CO$ to ethanol are fairly facile under the experimental conditions. Therefore, $CH_2CH_2O$ is very unlikely to be involved in ethanol synthesis on Rh(111).

**C. Microkinetic Modeling.** In section III.B, our DFT study showed that ethanol production on Rh(111) starts with HCO formation and the products involve $CH_4$, $CH_3OH$, $CH_3CHO$, and $C_2H_5OH$. Figure 4 summarizes the optimal reaction pathways for $C_2H_5OH$ synthesis on Rh(111) and the corresponding geometries of the transition states. All elementary steps involved in the optimal pathways are listed in Table 2, where the prefactors and reaction barriers for each step are also included. On the basis of these calculated potential energies, we took a further step to estimate the overall reaction rate and the rates for $CH_4$, $CH_3OH$, $CH_3CHO$, and $C_2H_5OH$ production under typical $C_2H_5OH$ synthesis conditions. To provide more accurate energies for the kinetic modeling, the reaction energies and barriers are ZPE-corrected (see Figure 4 and Table 2), which vary slightly from the non-ZPE-corrected results shown in Figures 1−3, while the energy differences from one step to the next are almost the same. To estimate the reaction rate, a microkinetic model was developed. The adsorption processes (**R1** and **R2**, see Table 2) were assumed to be in equilibrium. The slowest step among **R3**−**R13** was considered as the rls in the present microkinetic model.[46] One can see in Table 2 that, for $C_2H_5OH$ synthesis on Rh(111), the hydrogenation of CO (**R3**) to HCO is the rls with a barrier of 1.28 eV. For the minority species $CH_xO$ ($x$ = 1−3), $CH_3$, O, OH, $CH_3COH$, and $CH_3CHOH$, we applied the pseudo-steady-state approximation. That is, the rates for production and consumption of the species are the same, which are both controlled by the rls. A detailed description of the microkinetic model is given in the Supporting Information. Similar kinetic modeling approaches have been successfully applied for various reactions on metal and metal compound surfaces.[47−49]

**C.1. Ethanol Productivity and Selectivity.** On the basis of this microkinetic model and the DFT-calculated energies ($\Delta E$ and $E_a$), we are able to estimate the overall reaction rate ($r$) and the rates for $CH_3OH$ ($r_{CH_3OH}$), $CH_4$ ($r_{CH_4}$), $CH_3CHO$ ($r_{CH_3CHO}$), and $C_2H_5OH$ ($r_{C_2H_5OH}$) production (see the Supporting Information) under typical experimental conditions ($P_{CO}$ = 4 atm, $P_{H_2}$ = 8 atm, and $T$ = 523−623 K). Our results show that the overall reaction on Rh(111) is very slow and therefore the productivity to $C_2H_5OH$ is limited ($r_{total} = 4.5 \times 10^{-5}$ $s^{-1}$ $site^{-1}$ at 543 K). Due to the strong Rh−CO interaction, the surface is mainly covered by CO during the reaction; in contrast, H and other intermediates are much less. The relative selectivity of the products from the syngas reaction on Rh(111) at different temperatures is shown in Figure 5. Here relative selectivity is defined by the relative rate for each product, $r_i/(r_{CH_3OH} + r_{CH_4} + r_{CH_3CHO} + r_{C_2H_5OH})$, where $i$ is the species of the products. Our microkinetic modeling shows that $r_{CH_3CHO}$ is negligible compared to the other products, and therefore the selectivity for $CH_3CHO$ is not included in Figure 5. Our DFT results agree well with previous studies,[13,50] showing that $CH_3CHO$ is less dominant than $C_2H_5OH$, yet it is hard to avoid $CH_3CHO$ formation through the CO insertion mechanism. As seen in Figure 5, pure Rh(111) has relatively low selectivity for $C_2H_5OH$. The major product is $CH_4$, and the production of

(44) Chen, H.-L.; Liu, S.-H.; Ho, J.-J. *J. Phys. Chem. B* **2006**, *110*, 14816–14823.
(45) Chen, H.-L.; Peng, W.-T.; Ho, J.-J.; Hsieh, H.-M. *Chem. Phys.* **2008**, *348*, 161–168.
(46) Campbell, C. T. *J. Catal.* **2001**, *204*, 520–524.
(47) Liu, P.; A., R. J. *J. Chem. Phys.* **2007**, *126*, 164705.
(48) Liu, P.; Logadottir, A.; Nørskov, J. K. *Electrochim. Acta* **2003**, *48*, 3731–3742.
(49) Liu, P.; Rodriguez, J. A. *J. Phys. Chem. B* **2006**, *110*, 19418–19425.
(50) Du, Y.-H.; Chen, D.-A.; Tsai, K.-R. *Appl. Catal.* **1987**, *35*, 77–92.

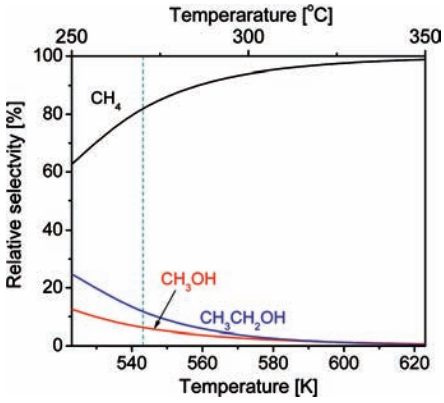


***Figure 5.*** Temperature dependence of the relative selectivity of major products from the syngas reaction on Rh(111) using the microkinetic modeling technique. The dashed line denotes a typical temperature for the syngas at 543 K.

$CH_3OH$ and $C_2H_5OH$ is much lower. This is consistent with the experiments, where the Rh catalysts seem to produce hydrocarbons only, independent of the support.[5,13,51,52] It should be noted that even though our microkinetic modeling describes well the reaction on a model Rh catalyst, it is known that the real Rh-based catalysts are always mixed with other promoters such as Fe or Mn and supports such as $SiO_2$, $Al_2O_3$, or $CeO_2$.[5−7,13] As demonstrated below, depending on the promoters and the supports, the coverage and adsorption energy of the adsorbates may change, which in turn would affect the reaction barrier and the modeling results.

**C.2. Factors To Control Ethanol Productivity and Selectivity.** Now, the questions are as follows: What controls the $C_2H_5OH$ productivity and selectivity on Rh? Are there any possible ways to improve them? To answer these questions, we performed a microkinetic analysis to identify the productivity- and selectivity-controlling factors by artificially and independently changing several variables in the kinetic model. The first changed variable is the CO adsorption energy, as the interaction of CO with the surface is very important to the whole reaction. What we did is to make the CO binding weaker by $\Delta E_{ads}$(CO). Here, we assume that the activation barriers are linearly correlated with the heat of reactions through the Brønsted−Evans−Polanyi (BEP) relation ($E_a = \alpha\Delta E + \beta$). With the decrease of CO binding, the heat of the reactions involving CO as a reactant is lowered by $\Delta E_{ads}$(CO) and the corresponding barriers are decreased by $\alpha\Delta E_{ads}$(CO). Here, $\alpha$ is the BEP correlation constant and $\alpha = 0.1$, as pointed out before for bond formation reactions.[53] Given that, weakening CO bonding not only will decrease the amount of CO on the surface (**R1**), therefore making more sites available for the reactions, but also will lower the barriers for the rls (**R3**) and for C−C bond formation (**R9**). Besides this variable, the others were kept the same. The purpose of this analysis is to understand the independent effect of each variable. Our results show that weakening the CO bonding does help productivity due to the decreased barrier for the rls (**R3**) and the increased H coverage, where 0.4 eV weakening of CO bonding strength leads to $r_{total}$ increased by a factor of $\sim 5 \times 10^3$ at 543 K. Yet the selectivity remains almost the same as that shown in Figure 5. It is likely that decreasing the CO−surface interaction accelerates the formation of each product almost equally, by increasing the amount of $CH_3O$ for $CH_3OH$ production (**R6**) and therefore the $CH_3$ for $CH_4$ production (**R8**) as well as $CH_3CO$ formation (**R9**), which leads to $C_2H_5OH$ production. Although the weaker CO bonding lowers the barrier for C−C bond formation (**R9**) by $\alpha\Delta E_{ads}$(CO), the decrease is very small by adopting $\alpha = 0.1$ and it does not help $C_2H_5OH$ selectivity. A similar analysis was also performed by increasing the H adsorption energy. The effect of changing H binding strength [$\Delta E_{ads}$(H)] on the barriers of hydrogenation steps (**R3**−**R6**, **R8**, and **R10**−**R15**) was also included by shifting the barriers of $\alpha\Delta E$(H) ($\alpha = 0.1$). Again, with a stronger H−surface interaction, the overall conversion increases, where 0.4 eV strengthening of the H bonding increases $r_{total}$ by a factor of ∼30 at 543 K. Again, no improvement of the selectivity was observed. Increasing the H binding energy has two opposite effects on the hydrogenation steps: one is facilitating hydrogenation via the increased H coverage, and the other is slowing down the associated processes due to increased barriers for hydrogenation by $\alpha\Delta E_{ads}$(H). In fact, our calculations show that increasing H coverage affects the overall rate much more than increasing the barriers for the hydrogenation processes. As a result, the rls (**R3**) becomes faster. Similar to the case of decreasing the CO binding energy, it also accelerates the formation of each product almost equally, by increasing the amount of $CH_3O$ (**R5**), $CH_3$ (**R6**), and $CH_3CO$ (**R9**). The increasing productivities of the three products including $C_2H_5OH$ were also observed when lowering the barriers for the rls (**R3**) and the formation of $CH_3O$ (**R5**). In addition, accelerating $CH_3$ formation (**R7**) as well as suppressing $CH_3OH$ production (**R6**) leads to a decreasing amount of $CH_3OH$ but an increasing production of $CH_4$ and $C_2H_5OH$. Therefore, all of these procedures help increase $C_2H_5OH$ productivity; however, none of them generates significant effects on the selectivity, where $CH_4$ is always a major product as shown in Figure 5.

According to our microkinetic analysis, there are only two variables that affect the $C_2H_5OH$ productivity as well as selectivity significantly. One is the barrier for $CH_4$ formation (**R8**); the other is the barrier for CO insertion or C−C bond formation (**R9**). As shown in Figure 6a, the selectivities for $CH_4$ and $C_2H_5OH$ cross each other upon increasing the barrier of $CH_4$ formation by only ∼0.1 eV. With that, much higher selectivity for $C_2H_5OH$ over $CH_4$ was observed. By suppressing the production of $CH_4$ (**R8**), more $CH_3$ will be available for the formation of $CH_3CO$ (**R9**), and therefore the $C_2H_5OH$ production increases. Alternatively, high $C_2H_5OH$ selectivity can also be achieved by lowering the barrier for formation of $CH_3CO$ (**R9**), as shown in Figure 6b. In this way, the $CH_4$ formation (**R8**) also cannot compete with $CH_3CO$ (**R9**) for the $CH_3$ resources and therefore more $C_2H_5OH$ is produced compared to $CH_4$. It should be noted that the increase in $CH_3OH$ selectivity together with $C_2H_5OH$ during both processes was also observed in Figure 6. However, the selectivity increase for $CH_3OH$ is much smaller than that for $C_2H_5OH$. Similar phenomena have also been observed experimentally when promoters such as Fe and Mn are applied for the Rh-based catalysts.[13]

Overall, our DFT calculations and microkinetic modeling show that $C_2H_5OH$ synthesis from CO and $H_2$ is feasible on pure Rh(111) via HCO, $CH_3O$, $CH_3$, and $CH_3CO$ intermediates. However, the efficiency of Rh(111) is low due to the strong CO−Rh interaction, resulting in CO poisoning and slow kinetics

(51) Iizuka, T.; Tanaka, Y.; Tanabe, K. *J. Catal.* **1982**, *76*, 1–9.
(52) Solymosi, F.; Tombácz, I.; Kocsis, M. *J. Catal.* **1982**, *75*, 78–93.
(53) Schumacher, N.; Boisen, A.; Dahl, S.; Gokhale, A. A.; Kandoi, S.; Grabow, L. C.; Dumesic, J. A.; Mavrikakis, M.; Chorkendorff, I. *J. Catal.* **2005**, *229*, 265–275.

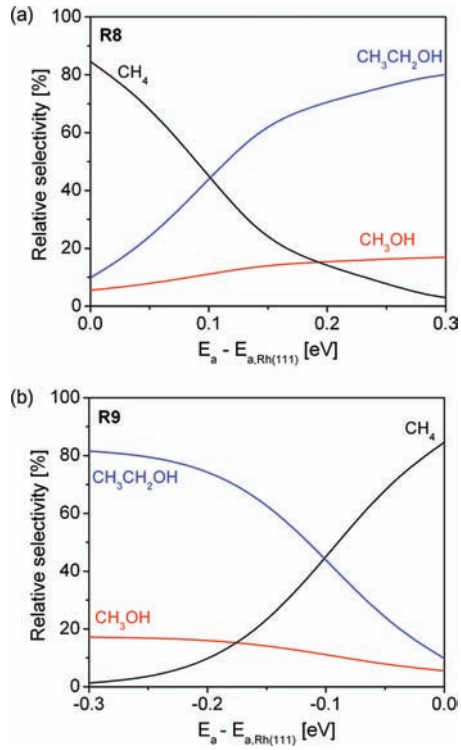


***Figure 6.*** Effects of variation of reaction barriers ($E_a$) for (a) $CH_3^* + H^* \rightarrow CH_4(g) + 2^*$ (**R8**) and (b) $CH_3^* + CO^* \rightarrow CH_3CO^* + *$ (**R9**) on the relative selectivity of major products from the syngas reaction on Rh(111) using the microkinetic modeling technique.

for the rate-limiting CO hydrogenation. In addition, Rh(111) is highly selective for $CH_4$ rather than $C_2H_5OH$. According to our microkinetic analysis, the $C_2H_5OH$ productivity of Rh can be improved by using promoters or supports that are able to weaken CO bonding, strengthen H binding, lower the barriers for hydrogenation and C−O bond breaking of $CH_3O$, and/or suppress $CH_3OH$ formation. There are only two possible ways to increase $C_2H_5OH$ productivity and selectivity. One is to suppress the formation of $CH_4$; the other is to facilitate C−C bond formation. Therefore, when Rh-based catalysts are developed for $C_2H_5OH$ synthesis, the catalytic activities of the materials toward $CH_4$ formation and C−C bond formation have to be especially considered. To achieve high $C_2H_5OH$ productivity and selectivity, promoters and/or supports used for Rh catalysts should minimize $CH_4$ production and/or maximize chain growth from $C_1$ oxygenates to $C_2$ oxygenates.

To validate our predictions, we took one simple example to examine the effect of Fe, which has been identified as one of the promoters for ethanol synthesis on Rh.[5−7,13] To set up the model, a Rh atom from the topmost layer of the Rh(111) surface was replaced by a Fe atom (Figure 7). Then CI-NEB calculations were carried out for the methane formation process, leading to a reaction barrier of 1.21 eV (non-ZPE-corrected, Figure 7). This is much higher than that on pure Rh(111), where the reaction barrier is 0.57 eV. Compared to the pure Rh(111) surface, the presence of Fe in the surface shifts the d-band center of Rh closer to the Fermi level by 0.20 eV, which helps stabilize the $CH_3$ species by 0.76 eV as well as the atomic H species by 0.1 eV,[54] while for $CH_4$ the effect is very small and the molecule still does not interact with the surface. Given that, our calculations show an increased barrier for methane formation upon

(54) Hammer, B.; Nørskov, J. K. *Adv. Catal.* **2000**, *45*, 71–129.

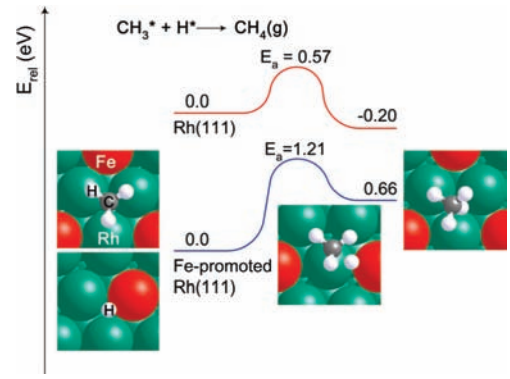


***Figure 7.*** Comparison of reaction barriers ($E_a$) and reaction energies ($\Delta E$) for the methane formation process, $CH_3^* + H^* \rightarrow CH_4(g) + 2^*$, on pure and Fe-promoted Rh(111) surfaces (large cyan, Rh; large red, O; small gray, C; small white, H).

going from Rh(111) to Fe-promoted Rh(111). According to our microkinetic modeling results in Figure 6a, the increased barrier for methane formation due to the Fe promoter should lead to methane suppression and therefore increased ethanol productivity as well as selectivity, which agrees well with the experimental observations.[5−7,13]

## IV. Conclusion

In the present study, $C_2H_5OH$ synthesis from syngas on Rh(111) has been explored by DFT calculations and microkinetic modeling. Our results show that, in accordance with the experiments on Rh-based catalysts,[5,7] three main products are involved in this process: $CH_4$, $CH_3OH$, and $C_2H_5OH$; in contrast, the production of $CH_3CHO$ is negligible. The reaction is started by HCO formation from CO hydrogenation, while the CO dissociation route is not energetically favored on Rh(111). The produced HCO species is then further hydrogenated to $CH_3O$, which eventually forms $CH_3OH$ via hydrogenation and $CH_3$ via dissociation. This is followed by the production of $CH_4$, via $CH_3$ hydrogenation, and of $CH_3CO$, via CO insertion or C−C bond formation, which is the key intermediate leading to the $C_2H_5OH$ formation. The rate-limiting step of the overall reaction is the first hydrogenation of CO to HCO. The strong Rh−CO interaction is an obstacle to CO hydrogenation and therefore slows down the overall conversion; however, its high affinity for $CH_3$, O, and $CH_3CO$ species indeed helps the C−O bond cleavage of $CH_3O$ species and makes direct ethanol synthesis possible. Our microkinetic modeling based on the DFT calculations clearly manifests that the overall conversion on Rh(111) is limited due to the strong CO−Rh interaction, which results in CO poisoning and slow kinetics for the CO hydrogenation.

In addition, Rh(111) is highly selective for $CH_4$ rather than $C_2H_5OH$ or $CH_3OH$. The overall reaction rate and therefore the $C_2H_5OH$ productivity can be increased by weakening CO bonding, strengthening H binding, lowering the barriers for hydrogenation and C−O bond breaking of $CH_3O$, and/or suppressing $CH_3OH$ formation. The productivity and selectivity for $C_2H_5OH$ are only controlled by $CH_4$ formation and C−C bond formation between $CH_3$ and CO. Our results show that to achieve the high $C_2H_5OH$ productivity and selectivity, promoters and/or supports to the Rh are necessary, which should help minimize $CH_4$ production and/or facilitate chain growth from $C_1$ oxygenates to $C_2$ oxygenates. The validity of our prediction is proved by a simple test to understand the promoting effect of Fe toward ethanol synthesis on Rh. Our results show that

the presence of Fe helps stabilize $CH_3$ and atomic H species, which suppresses methane formation and therefore increases ethanol productivity as well as selectivity.

**Acknowledgment.** This research was carried out at Brookhaven National Laboratory under Contract DE-AC02-98CH10886 with the U.S. Department of Energy (Division of Chemical Sciences). First-principle calculations were carried out using computational resources at Center for Functional Nanomaterials, Brookhaven National Laboratory, and National Energy Research Scientific Computing Center, which is supported by the Office of Science of the U.S. Department of Energy under Contract DE-AC02-05CH11231. We appreciate Dr. Peter Ferrin and Professor Manos Mavrikakis for providing activation energies for C−C and C−O bond-breaking in ethanol.

**Supporting Information Available:** Detailed information on microkinetic modeling, optimized geometries, and energies. This material is available free of charge via the Internet at http://pubs.acs.org.

JA903013X